# FREEFORM SURFACES USING ARCHITECTURAL SPANISH PATTERNS FROM THE MIDDLE AGE

**Natalia CAICEDO-LLANO**
Assistant Professor, PhD, Universidad Tecnológica Metropolitana, Faculty of Ciencias de la Construcción y Ordenamiento Territorial, Department of Planificación y Ordenamiento Territorial, e-mail: ncaicedo@utem.cl

**Suzanne SEGEUR-VILLANUEVA**
Assistant Professor, PhD Candidate, Universidad Politécnica de Valencia, Escuela de Arquitectura, Departament of Construcciones Arquitectónicas, e-mail: susevil1@doctor.upv.es

**Abstract**. We present an optimization of an interlaced structure that has as starting geometry a Spanish pattern from the middle age to create freeform surfaces. As well we present an optimization of an interlaced structure that has as starting geometry a combination of two patterns to create single curved surfaces. First, we compare some representation methods to transform flat patterned surfaces into freeform surfaces. We recommend the most appropriate method for different types of surfaces such as: vaults, domes, half spheres, saddles, and ripped surfaces. The intent is to use the method that allows keeping as many equal jigs as possible. Second, as the interlaced structures have the capacity of keeping continuity between two different patterns on one direction, we established a method to divide a surface according to a criterion and we create interlaced structures with different density on each region. The pattern is selected based on the density that better suits the region.

**Key words**: morphologic algorithms, interlaced geometries, structures, vernacular revival

## Introduction

The aim of this paper is to apply constructive concepts in the generation of freeform structures based on a treatise written by Diego López de Arenas (1912) for the construction of timber interlaced carpentry. First, standardization of items is an advantage of this type of structure. Second, been able to cover a big span using small section of timber allows the use of species that usually do not have structural applications. It is not only a geometrical transformation but also a selection of a method allowing creating as many equal jigs as possible, same criteria than the one used in (Brocato and Mondardini, 2012), and in (Tanguy *et al.*, 2014). Also, the interlaced carpentry makes possible the construction of a structure with a big span using small battens, criteria

also taken in consideration in (Brocato and Mondardini, 2015), in (Baverel and Nooshin, 2007), and in (Burry *et al.*, 2012). At the same time it is use for decoration because of its beauty. Some contemporary buildings, like the ones designed by Shigeru Ban are inspired by Mudejar carpentry. Even if they are entirely computerized, to be manufactured they require a completely CNC machining because they lack of a geometric optimization. Examples of it are: the Yeoju Golf Club and the Pompidou of Metz (Balinski and Januszkiewicz, 2016). According to López de Arenas (1912), only for flat surfaces, it is possible to build a very large number of geometries, with a reduced number of rafter squares. On the opposite, very few freeform surfaces have been constructed in that period of time because of the large number of rafter squares required and manufacturing difficulties. An example of a half-sphere built is at the convent of San Francisco in Lima, where the geometric transformation chosen (see the description on the section 4.1) has as consequence a difficult and expensive type of construction. Timber, the material chosen by Spanish carpenters for this type of construction has also some characteristics that need to be taken in consideration. Each species has a different Young modulus and compression stress resistance, mechanical characteristics related with its capacity for bowing applications (Caicedo-Llano, 2014). In this case, timber is cut following an arc, instead of been bowed, not considering that timber is an anisotropic material, where longitudinal properties are different from radial or tangent ones. When working with timber, it is recommended to use as much longitudinal fibers as possible to take advantage of mechanical properties of the material (Aicher *et al.*, 2001).

The intent of this paper is to demonstrate, for freeform surfaces, how a reduction of the number of different jigs can be done through an optimization of geometric algorithms. A geometric optimization can be reached through practical experimentation or through a theoretical approach. Some theoretical approaches where geometric optimization is used to reduce the cost of manufacturing are: the mesh segmentation driven by Gaussian curvature (Yamauchi *et al.*, 2005), and how joints can be improved to resist bending forces thanks to morphological algorithms (Weinand *et al.*, 2017).

## 1. Methodology

All figures are generated in the software "Rhinoceros 5.0", excluding the Fig. 27 that is a photograph taken by our own. Complex figures are generated writing a code in the plug-in "Grasshopper" of "Rhinoceros 5.0.". Codes were run many times to have different results varying the input. For the purpose of this article, inputs are Cartesian equations of geometries. Some exceptions like figures in sections 4.5, 4.8, and 5.0 we generated with the same software ("Rhinoceros 5.0.") adding the plug-in "Paneling tools" instead. Equations are the results of our own experimental work. The parameters used to generate the examples are taken with the purpose of having flagrant curvatures where differences can be easily observed.

## 2. Interlaced structures in Spanish historic carpentry

According to Nuere (1989), based on the treatise of López de Arenas and other treatises from that period, explains the technique to construct interlaced carpentry. This type of carpentry, according to him, cannot be considered as a derivation of Mudejar carpentry from the Middle East but as a new type or carpentry created in Spain.

Interlaced carpentry, in Spanish "carpintería de lazo" means a carpentry made of bows. It is defined also as a combination of "wheels", in Spanish "ruedas", as an analogy between the wheel used in mechanics and the wheel drawing method based on the rotation of lines having a point as center. We choose four combinations of wheels. Criteria for the selection are: a different number of points in the wheel, and a different ratio between wheels. In consequence there are patterns that can be inscribed in triangles, squares, diamonds and rectangles, having orthogonal and non-orthogonal patterns and a representative sample of the total possible combinations.

In the Fig. 28, is illustrated the method to draw a wheel of eight points described in (Nuere, 1989). The method starts by drawing an arbitrary octagon having as center the intersection of $x$ and $y$ axis, as in the Fig. 28 (in the upper-left corner). The midpoint of each edge intersects endpoints of a star of forty-five degrees, as in Fig. 28 (at the top center). Then, from an endpoint of this octagon, a circle must be drawn having as radius the closest endpoint of the star of forty-five degrees, as in the Fig. 28 (in the upper-right corner). The circle intersects the $x$ axis in two points. Choose the furthest point to the center of the octagon as the vertex of a second octagon, as in the Fig. 28 (in the lower-left corner). Then lines from the star are extended until the second octagon, as in the Fig. 28 (at the bottom center). In the Fig. 28 (in the lower-right corner) are erased: the first octagon, and in an alternate way the second octagon having as reference, lines extended in the Fig. 28 (at the bottom center).

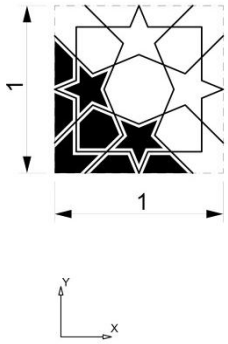


**Fig. 1**. Pattern based on a wheel of eight points.

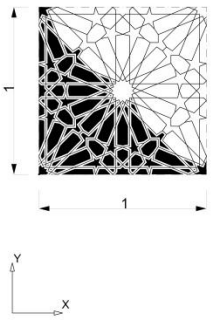


**Fig. 2**. Pattern based on a wheel of eight points and a wheel of sixteen points.

When the previous wheel is placed side by side, it creates a pattern called from now on, a "pattern of wheels of eight points", as in the Fig. 1. The method to draw any other wheel is similar to draw a wheel of sixteen points; the method is to start by drawing a hexa-decagon instead of an octagon. A pattern based on a wheel of

eight points and a wheel of sixteen points is a combination of wheels of eight points and wheels of sixteen points placed in an alternate way, as in the Fig. 2.

In the Fig. 3 is shown a pattern based on a wheel of ten points. In the middle age it was possible to draw with rafters squares of seventy-two degrees and eighteen degrees respectively.

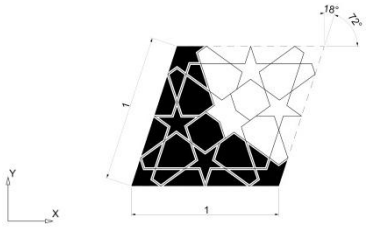

**Fig. 3**. Pattern based on a wheel of ten points.

In the Fig. 4 is shown a pattern of wheels of nine points and wheels of twelve points.

To conclude, these interlaced structures could be built in the middle age with few rafters squares for each type of wheel. Thereafter, we will show how this advantage will be understood as a possibility to build a limited number of jigs of battens and assemblages for freeform surfaces.

## 3. A flat patterned surface topologically deformed into single curved surfaces

### *3.1. A flat patterned surface topologically deformed into a vault*

We consider a flat surface with a pattern of wheels of eight points. We do a topological deformation of this surface. This method can be applied for surfaces with vanishing Gaussian curvature and can therefore be unfolded to the plane without distortions (Glaeser and Gruber, 2007), and (Hoschek, 1998). We have as final configuration the surface shown in the Fig. 5 with the following Cartesian equation:

$$x^2 + z^2 = \sqrt{2.8} \qquad \text{Equation 1}$$

where,

$$\begin{cases} -1.8 \leq x \leq 1.8 \\ -2.8 \leq y \leq 2.8 \end{cases}$$

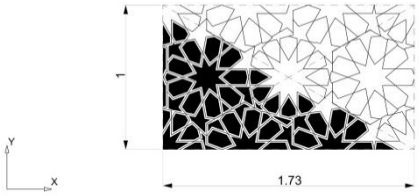


**Fig. 4**. Pattern based on a wheel of nine points and a wheel of twelve points.

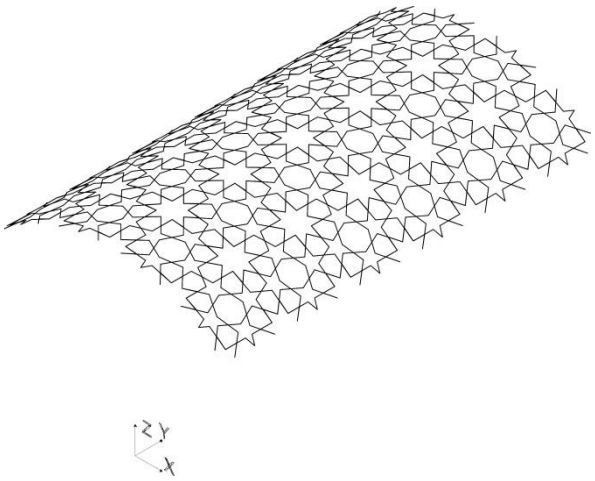

**Fig. 5**. Topological deformation of a pattern of a wheel of eight into a vault.

This method is useful when deforming a pattern that takes the geometry of a vault. The flat surface has the same number of jigs than the vault.

### *3.2. A flat patterned surface topologically deformed into an elliptical vault*

We consider a flat surface with a pattern of wheels of eight points. We

do a topological deformation of this surface and we have as final configuration the surface shown in the Fig. 6 with the following Cartesian equation:

$$\frac{x^2}{2.5^2}+\frac{z^2}{4^2}=1 \qquad \text{Equation 2}$$

where,

$$\begin{cases} -2.5 \leq x \leq 2.5 \\ -2.57 \leq y \leq 2.57 \end{cases}$$

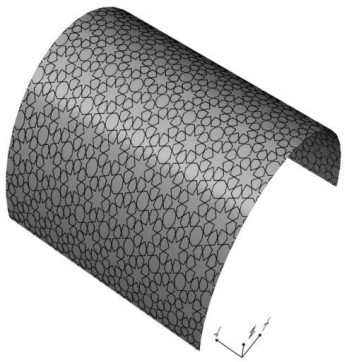

**Fig. 6**. Topological deformation of a pattern of a wheel of eight into an elliptical vault.

With the aim of comparing the difference between the lengths of battens in relation with the surface, we introduce a criterion called the relative error *R*. It is calculated as per the following equation:

$$R=\frac{L_{max}-L_{min}}{L_s} \qquad \text{Equation 3}$$

where, $L_{max}$ is the maximal length of the batten, $L_{min}$ is the minimal length of the batten, and $L_s$ is smallest span of the surface. For the selection of $L_{max}$ and $L_{min}$ we exported to the software "Excel" a list of lengths of battens per figure. Then, the list was split in categories (depending on the number of types of battens). We selected the maximal and minimal length of the longest type of batten.

From now on, to be able to compare methods easily, we consider battens placed at the periphery as standards jigs, even in the practice they are different ones.

In this case, the relative error *R* should be bigger than $10^{-2}$ in order to have two jigs of battens to build the elliptical vault including battens connecting wheels between them. To conclude, considering single curved surfaces, when the radius of curvature is constant, for example the vault, the number of jigs is equal than the number of jigs of a flat surface. When the radius of curvature varies, for example the elliptical vault, the number of jigs could be higher than the number of jigs of a flat surface; depending on the relative error required.

## 4. A flat patterned surface transformed applying different methods on freeform surfaces

### *4.1. Generation of a dome applying the polyhedral method using a dodecagonal pyramid as starting geometry*

We recommend the use of the following representation methods for domes. First, we generate a half Archimedean polyhedron based on a pattern, and then we project it to a dome. The Archimedean polyhedron has the same number of vectors directors than the number of segments of the pattern. Each segment is projected to the dome having a vector director that starts at the center of the sphere (where the dome can be inscribed) and ends at the midpoint of each segment.

We consider a triangle with a pattern of wheels of eight points because is one

of the simplest patterns (as in the Fig. 7). We do twelve polar arrays based on the *z-axis* to have as result a dodecagonal pyramid (as in the Fig. 8). Then we project each segment to the dome inscribed in the dodecagonal pyramid having as vector director the center of the dome and the midpoint of each segment.

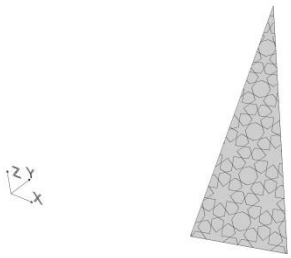

**Fig. 7**. A flat triangle with a pattern of a wheel of eight points of as starting geometry.

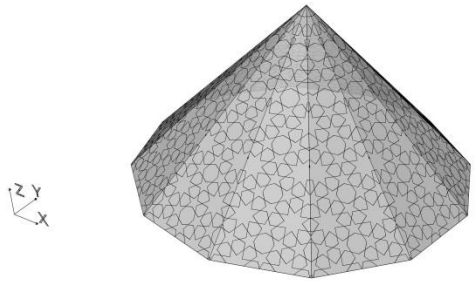

**Fig. 8**. Transformation of the triangle shown in the Fig. 7 in a dodecagonal pyramid through rotation.

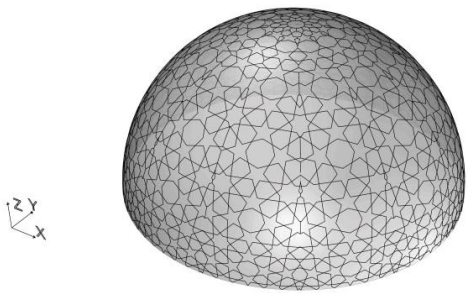

**Fig. 9**. Projection of the dodecagonal pyramid shown in Fig. 8 to a dome.

This procedure is also known as the quarter method, method described in (Huerta, 2007), and in (Mark, 1996). It has as consequence a large number of different jigs and many difficulties to manufacture joints at intersections of quarters (as in the Fig. 9).

### *4.2. Generation of a dome applying the polyhedral method using a half-truncated cube as starting geometry*

We consider a pattern of wheels of eight points because is the simplest pattern. The more appropriate polygon to create a wheel of eight-point pattern is an octagon. From all Archimedean polyhedron, only the truncated cube and the truncated cuboctahedron have octagon faces.

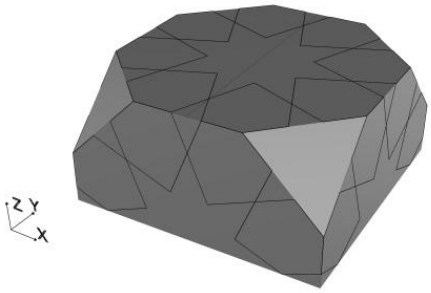

**Fig. 10**. Generation of a half-truncated cube using a flat surface with a pattern of a wheel of eight points of as starting geometry.

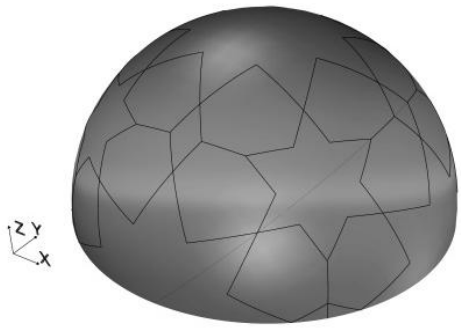

**Fig. 11**. Projection of the half-truncated cube shown in the Fig. 9 to a dome.

In the Fig. 10 is shown a half-truncated cube based on a pattern of a wheel of eight points. The method established to generate any dome is selecting the more convenient polygon based on a

particular pattern and its corresponding Archimedean polyhedron.

In the Fig. 11 is shown the projection of segments from the half-truncated cube to a dome. A half-truncated cube has one octagon, four half octagons and four triangles. With a pattern of eight points on each face there are ninety-two elements in total. To conclude, the half-truncated cube and the projected dome can be built with only six jigs of battens without a relative error, including battens placed at the periphery. In conclusion, with this transformation method, we can manufacture a freeform surface with the same number of jigs than a flat surface with the same pattern.

### *4.3. A flat patterned surface topologically deformed into a half-sphere*

We consider a flat surface with a pattern of wheels of ten points. We do a topological deformation of this surface and we have as final configuration the surface shown in the Fig. 12 with the following Cartesian equation:

$$x^2 + y^2 + z^2 = 2 \qquad \text{Equation 4}$$

where,

$$\begin{cases} -2 \leq x \leq 2 \\ -2 \leq y \leq 2 \\ 0 \leq z \leq 2 \end{cases}$$

To conclude, in this case, the relative error $R$ should be bigger than $10^{-1}$ in order to have three jigs of battens to build the half sphere including battens connecting wheels between them.

### *4.4. Generation of a half-sphere using a flat patterned surface as starting geometry applying the compass method point by point for each wheel*

The compass method as in Otto *et al.* (1974) allows the creation of a grid of rhombus on an ordinary surface using only a compass, as shown in the Fig. 29. This method is also described in (Bouhaya *et al.*, 2014), and in (Lefevre *et al.*, 2015).

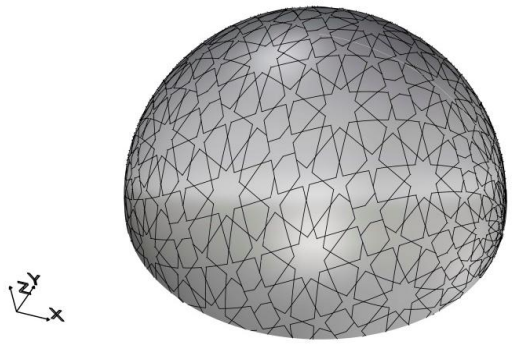


**Fig. 12.** Topological transformation of a pattern of a wheel of ten points into a half-sphere.

To simplify, we consider a plane where two guidelines are arbitrary chosen. A step of the grid is as well arbitrary chosen, been also the radius of the compass. Starting at the intersection point *O*, intersection of guidelines, the first guideline is divided with the compass naming *An* (where *n* is a mathematical integer series) each intersection point. Starting at point *O*, the second guideline is divided with the compass naming *Bn* intersection point. We trace a circle centered in *C1*, point of intersection between circles centered in *A1* and *B1* and that correspond to the fourth point of the first rhombus. The intersection between the circle centered in *A2* and the circle centered in *C1* is named *C2*. This procedure is repeated as many times as needed in order to fill the surface to create a grid. For freeform surfaces, we use the same method but instead of drawing circles in a plane, we draw spheres on a freeform surface.

We consider the same half-sphere surface shown in the Fig. 12. The method

of the compass method point by point for each wheel is described as follows:

1. Take two arbitrary references planes (*xy*) and (*yz*) and give the name *A0,0* to the intersection point between the half-sphere surface and both reference planes. The notation code given to each point, from now on, is: *Xnx;ny*, where *X* is a letter starting with the first letter of the abecedary, *n* is a mathematical integer series and *x* and *y* are +1 or -1 depending on the position of the point in relation with the Cartesian coordinates system. Apply the compass method explained previously to create a grid of rhombus with a step *p* shown in the Fig. 13.
2. Select alternate points, more specifically points with the notation *A2nx;2ny*. In the Fig. 14 is shown the final configuration, note that points are different when creating a grid of rhombus with a step equal to *2p*.
3. Make the intersection between spheres with center *A0,0* and *A2nx;2ny* with a radius equal to the step *p* and the starting geometry, in this case the half-sphere surface. Intersections are circles where external octagons of the wheel of eight points are inscribed.
4. Take in consideration the four closets points between each other with notation *A2nx;2ny* that are also the quadrants of circles and divide arcs between points in two equal arcs. Middle points and endpoints become vertex of external octagons of the wheel of eight points. Name new points following the notation code: *Bnx;ny*.
5. Make spheres having as center the closest eight points named *A2nx;2ny* and *Bnx;ny* with an arbitrary radius named *r*. Then intersect previous spheres with the first circle obtaining sixteen points. Join opposite points in relation with the central symmetry considering the point *A0,0* as the center of symmetry. Project previous segments in to starting geometry having as vector director the center of the starting geometry *O0,0* and the center of each segment.

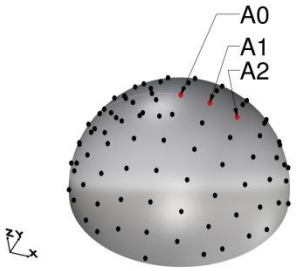


**Fig. 13**. Grid of rhombus in a half-sphere applying the compass method with radius *p*.

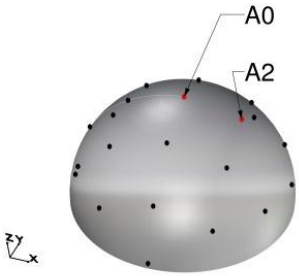


**Fig. 14**. Selection of alternate points of points shown in the Fig. 13.

6. Make intersection points between previous arcs and name external intersections points following the notation code: *Enx;ny,* and internal intersection points following the notation code *Fnx;ny*.
7. With the aim of respecting proportions of interlaced structures in flat surfaces explained in section 1, for freeform surfaces, make a sphere with center *F0;1*. Proportion is respected when the sphere intersect simultaneously points

*A0;1*, *E-1;2* and *E1;2*. After many loops modifying radius $r_a$ size, we find the best position for the point *F0;1*.

8. Make spheres with center *A-1;0* and *A1;0* with a radius equal to $r_a$. Then intersect them with the circle of center *A0,0*. Join opposite points in relation with the central symmetry considering the point *A0,0* as the center of symmetry. Project previous segments in to staring geometry having as vector director the center of the starting geometry *O0,0* and the center of each segment.
9. Join points with their closest points belonging to the circle with center *A0,0*. Project previous segments in to starting geometry having as vector director the center of the starting geometry and the center of each segment.

Repeat this method for each point with notation code *A2nx;2ny*. In the Fig. 15 is shown the final configuration when applying the method of the compass method point by point for each wheel based on a pattern of a wheel of ten on a half-sphere.

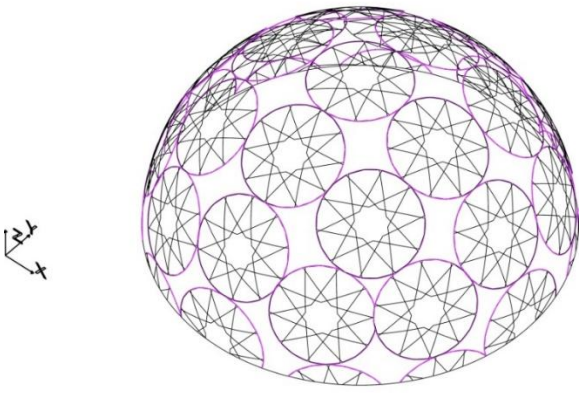

**Fig. 15**. Interlaced structure applying the compass method point by point for each wheel of ten points in a half-sphere.

To conclude, in this case, the relative error *R* should be bigger than $10^{-3}$ in order to have three jigs of battens and circles to build the half-sphere excluding battens connecting wheels between them.

### *4.5. Generation of a half-sphere using a flat patterned surface as starting geometry applying the paneling method*

We consider the half-sphere surface shown in the Fig. 12. We assign the pattern of wheels of sixteen and eight points to each rhombus (as in the Fig. 16). This method is described in (Rörig *et al.*, 2014) and it is applied in (Duro-Royo *et al.*, 2015). We project segments in to the half-sphere having as vector director the center of the sphere and the midpoint of each segment. We extend curves to join closest curves. In the Fig. 17 is shown the final configuration.

**Fig. 16**. Pattern of a wheel of sixteen and eight points assign to panels belonging to a half-sphere.

**Fig. 17**. Projection of panels on the half-sphere.

To conclude, in this case, the relative error *R* should be bigger than $10^{-3}$ in order to have 4 jigs to build the half-sphere including battens connecting wheels between them.

### *4.6. A flat patterned surface topologically deformed into a saddle*

We consider a flat surface with a pattern of wheels of ten points. We do a topological deformation of this surface and we have as final configuration the surface shown in the Fig. 18 with the following Cartesian equation:

$$z = \frac{x^2}{8} - \frac{y^2}{4.5} \qquad \text{Equation 5}$$

where,

$$\begin{cases} -6.115 \leq x \leq 6.115 \\ -4.22 \leq y \leq 4.22 \end{cases}$$

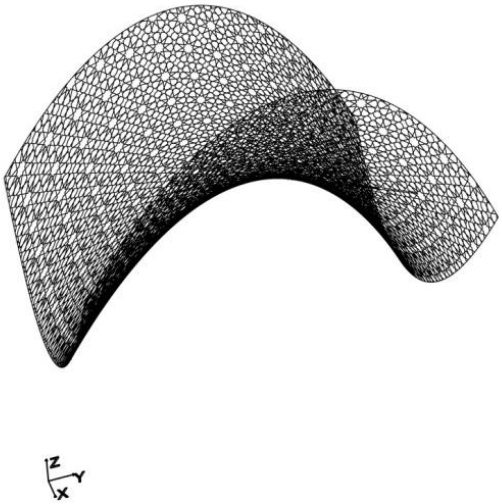

**Fig. 18**. Topological transformation of a pattern of a wheel of ten points into a saddle.

To conclude, in this case, the relative error *R* should be bigger than $10^{-2}$ in order to have three jigs of battens to build the saddle including battens connecting wheels between them.

### *4.7. Generation of a saddle with a pattern as starting geometry applying the compass method point by point for each wheel*

We consider the saddle surface shown in the Fig. 18. We create a grid of parallelograms with a step equal to two units, having as guidelines, intersections of planes (*xz*) and (*yz*) with the saddle. We apply the same method than in section 4.4., only modifying the vector director of the projection. Instead of having *O*0,0 the first point of the vector director and the point M the center of the segment with coordinates ($x_m$; $y_m$; $z_m$), the origin point is different for each segment. For each point *Mnx;ny*, the Cartesian equation of the parabola passing through the saddle is:

$$z = 0.1316\, x_m{}^2 \qquad \text{Equation 6}$$

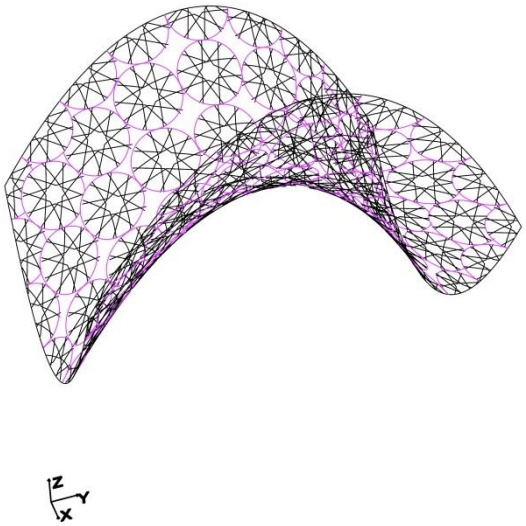

**Fig. 19** Interlaced structure applying the compass method point by point for each wheel of ten points in a saddle

Knowing that the focus of this parabola has coordinates (*0; $y_m$; $z_m$-1,9*), in order to do the projection of segments into the starting geometry, we project each segment following the vector director ($x_m$, *0*, $z_m$ *+1.9*).

In the Fig. 19 is shown the final configuration of this method.

To conclude, in this case, the relative error $R$ should be bigger than $10^{-3}$ in order to have seventeen jigs of battens and circles to build the saddle excluding battens connecting wheels between them.

### *4.8. Generation of a saddle with a pattern as starting geometry applying the paneling method*

We consider the saddle surface shown in the Fig. 18. To be consistent with the previous pattern selected, we transform a pattern of wheels of ten points. Been a pattern inscribed in a rhombus (as in the Fig. 3), in consequence we will explain the paneling method for a non-orthogonal grid as follows:

1. Place the starting point as the intersection of: 1.) the plane ($xz$), 2.) the 72° rotation of the plane ($xz$), and 3.) the saddle.
2. Apply the compass method described in the section 3.4. to make a first row of parallelograms with step $a$ (in this case equal to 2 units). Then we do a step $b$, approximately $\frac{2}{\tan 72°}$ (in this case equal to 0.62 units).
3. Take this point as starting point to create the second row of parallelograms. Continue using the same method for the following rows.
4. When creating panels from the non-orthogonal grid, you have to modify the width of the panel according to the original width (in this case equal to 2 units) instead of the original width plus the step $b$ (in this case equal to 2.62 units).
5. Project segments using the same method described in section 3.6.

In the Fig. 20 is shown the final configuration. To conclude, in this case, the relative error $R$ should be bigger than $10^{-2}$ in order to have three jigs to build the saddle including battens connecting wheels between them.

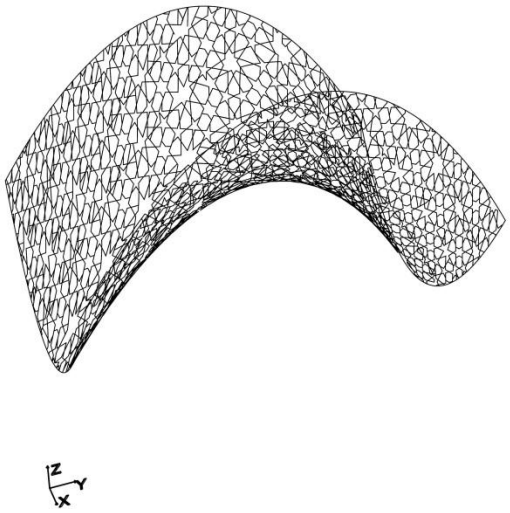


**Fig. 20**. Generation of a saddle surface with a pattern of wheel of ten points as starting geometry applying the paneling method.

To conclude, considering freeform surfaces, more specifically domes, the quarter method is not recommended because it has as consequence a large number of different jigs, the polyhedral method allows to have the same number of jigs than in a flat surface. Considering freeform surfaces with an orthogonal pattern like half-spheres or saddles, the number of jigs could be higher than in a flat surface, depending on the relative error $R$, criterion to sort methods, introduced previously. Comparing final configurations of the saddle applying the three methods (topological deformation, the compass method point by point for each wheel, and the paneling method), we conclude that if the relative error required is the same, the method allowing to have a smaller number of different jigs is the paneling

method. Considering freeform surfaces with a non-orthogonal pattern, the size of the step *b* (described previously), depends on the mean curvature of the surface. For this reason, the method has to be adapted stately depending on the type of surface and its mean curvature.

## 5. Generation of a single curved surface having a combination of patterns as starting geometry

### *5.1. The elliptical vault*

One of the advantages of the interlaced structure is to be able to change from a low-density pattern to a high-density pattern keeping the continuity of some elements. This is only possible when patterns of low and high density are proportional in terms of the number of points of the wheel. This combination of patterns is limited to single curved surfaces because pattern only match in one direction. We analyze how to interlace different patterns base on the geometry of the surface. The method used is the paneling method.

We consider the elliptical vault surface shown in the Fig. 6. Its Mean curvature is minimal at the springer and maximal at the keystone. The following equation allows knowing the radius of curvature *r* of the ellipse at any point:

$$r = \frac{(a^2 - \left(\frac{a^2 z^2}{b^2}\right) + (z - f)^2)(a^2 - \left(\frac{a^2 z^2}{b^2}\right) + (z + f)^2)^{0.75}}{ab}$$

Equation 7

where, *a* is the semi-minor axis (in this case 2.5), *b* is the semi-major axis (in this case 4), and *f* the focus $f = \sqrt{b^2 - a^2}$.

Arbitrarily, we decided to split the elliptical vault in two regions, one when the radius is larger than 2 units, and one when the radius is lower than 3 units. In order to find the value of *z* when the radius is equal to 2 units, we have to apply Equation 8:

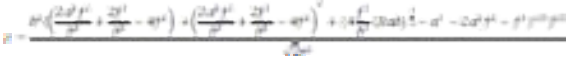

Equation 8

Where,

$z = 2.5$

In the Fig. 21 is shown a Mean curvature analysis of the surface. Its method is described in **(**Callens and Zadpoor, 2018). In regions of the surface of range $0.4 \leq z \leq 2.5$, we decided to adapt a pattern of high density (made of wheels of eight points). In the region of the surface with the range 2.5<*z*<4, where the radius of curvature is small and the mean curvature is high, we adapt a pattern of low density (made of wheels of sixteen points and wheels of eight points). We decide to do in the region close to the keystone a pattern of low density because battens of the structure have to be flexible in order to get a better adaptation to the geometry. From a geometrical point of view, we want to increase the relation between the length of battens and the radius of curvature of the elliptical vault, in order to reduce bowing efforts.

Once we assigned a type of pattern to each panel we project each segment into the surface. Knowing that points F, focus of arcs of ellipses composing the surface have as coordinates (*0, $y_m$, +3.12*), we project each segment following the vector director (*$x_m$, 0, $z_m$ - 3.12*) into the surface.

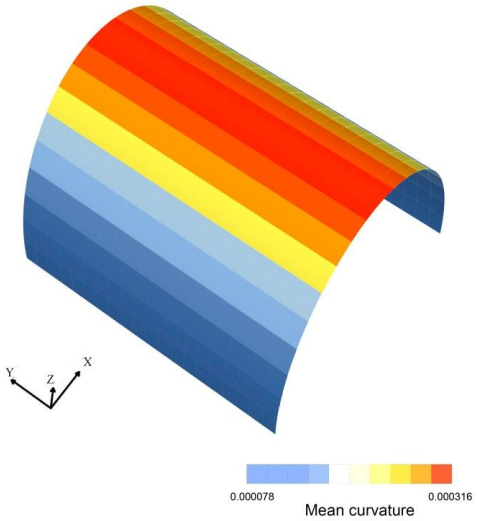


**Fig. 21**. Mean curvature of the surface with the Equation 9.

In the Fig. 22 and the Fig. 23 it is shown the final configuration of a combination of two patterns (a pattern of wheels of sixteen and eight points and a pattern of wheels of eight point) applying the paneling method in an elliptical vault.

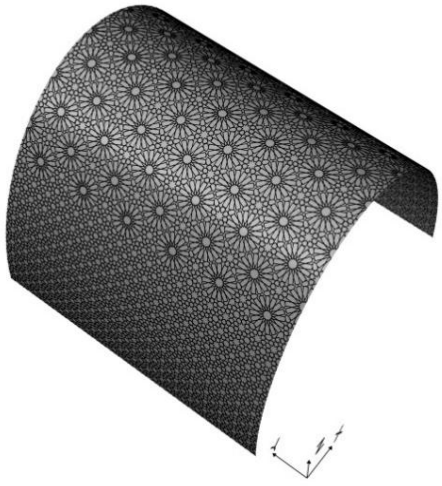

**Fig. 22**. Combination of two patterns applying the paneling method in an elliptical vault.

To conclude, in this case, the relative error *R* should be bigger than $10^{-4}$ in order to have five jigs to build the vault including battens connecting wheels between them.

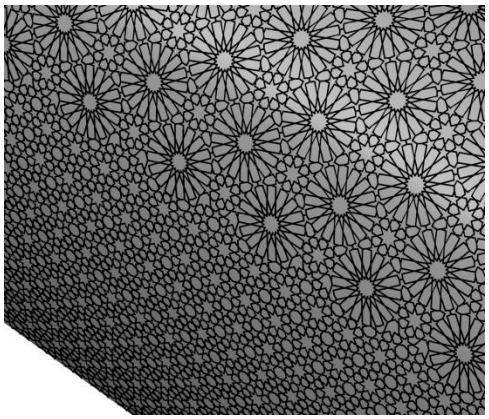

**Fig. 23**. Detail of a combination of two patterns applying the paneling method in an elliptical vault.

### *5.2. The rippled surface*

With the aim of researching about the usage of this method on a rippled surface, we consider the following Cartesian equation:

$$z = \sin x \qquad \text{Equation 9}$$

Where,

$$\begin{cases} -3.14 \leq x \leq 6.28 \\ -2.3 \leq y \leq 2.3 \end{cases}$$

Its Mean curvature is maximal at troughs and the crest, and is minimal at the rest of the surface. The following equation allows knowing the radius of curvature *r* of the ellipse at any point:

$$r = \frac{(\cos x^2)^{\frac{3}{2}}}{\sin x} \qquad \text{Equation 10}$$

Arbitrarily, we decided to separate the rippled surface in two regions, one when the radius is larger than ten units, and one when the radius is lower than ten units. In order to find the value of *z* when the radius is equal to ten units, we have to apply the following equation:

$$r = \left(-\frac{4}{\sin^2 x} + 6\,sin^2 x - sin^3 x\right)^{0.5} \qquad \text{Equation 11}$$

Where,

$x = -0.27 + \pi n; x = 0.27 + \pi n,$

In the Fig. 24 is shown a mean curvature analysis of the surface.

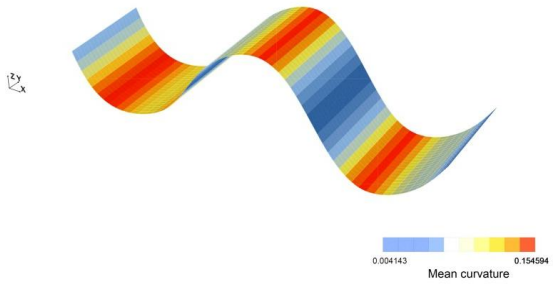


**Fig. 24**. Mean curvature of the surface of the Equation 9.

In the Fig. 25 and the Fig. 26 we decided to adapt a pattern of high density in regions of the surface of range $-1 \leq z \leq -0.27$ and $0.27 \leq z \leq 1$, and we adapt a pattern of low density in the region of the surface with the range -0.27<$z$<0.27, with the same criterion than in the section 5.1.

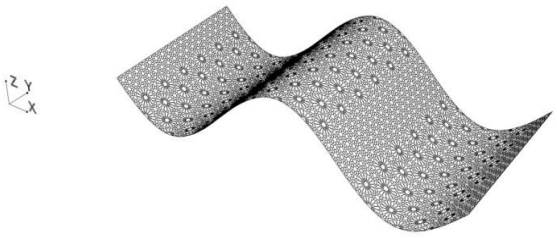

**Fig. 25**. Combination of two patterns applying the paneling method in a rippled surface.

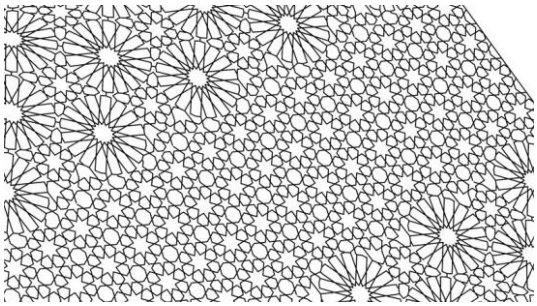

**Fig. 26**. Detail of a combination of two patterns applying the paneling method in a rippled surface.

To conclude, in this case, the relative error $R$ should be bigger than $10^{-3}$ in order to have five jigs to build the vault including battens connecting wheels between them. No matter what type o single curved surface, for a combination of two patterns from the middle age in Spain, with a small relative error required, we have as result, a small number of different jigs.

## 6. From the theory to the practice

In the Fig. 27 is shown a part of a half-sphere with a pattern of wheels of eight points using the transformation shown in the section 4.5. The prototype has a radius of curvature of two meters, inscribed in a frame of two by two meters, viewed in plan. The prototype is built in the south of France as part of a workshop at the "Grands Ateliers de l'Isle d'Abeau". For this reason, the French species that better suits for bowing applications is the European beech (*Fagus sylvatica*) (Peck, 2006), and (Buchelt and Wagenführ, 2008). Connectors are 3D printed with ABS (Acrylonitrile butadiene styrene) with steel caps.

We have modified the type of joints used by Spanish carpenters (tenon joints) with the purpose of having: 1) better mechanical properties by keeping the amount of timber or by not piercing it, 2) and a faster constructive system by simplifying the amount of work done on battens (that are largest elements that require an expensive cost of CNC manufacturing), and maximizing the number of equal jigs for battens and connectors. When the difference between battens is superior to a

relative error *R* equal to $10^{-3}$ (or three mm in this case), we consider battens as two different jigs. For mechanical reasons, we increased the number of battens between wheels in comparison with the geometry shown in Fig. 17 to be able to have approximately the same distance between battens everywhere. In total, the prototype has one hundred and twenty-eight timber battens with only eleven jigs, one hundred and sixty-eight ABS connectors with only twenty-five jigs, and three hundred and thirty-six steel caps with only one jig.

**Fig. 27**. Prototype of a freeform surface base on a pattern of a wheel of eight points.

The purpose to build the prototype is to locate main problems in order to focus future researches on improving the quality of the structure. The real geometry, also known as the final geometry is different from the nominal geometry. In the Fig. 30 and the Fig. 31 we make a visual comparison between the real geometry and (in pink) the nominal geometry (in black). The real geometry has been modeled based on a survey of the prototype shown in the Fig. 27. We observed in the Fig. 31, that the curve of the real geometry has a smaller curvature in the central left quarter area and has a larger curvature in the central write quarter area. The phenomenon is called buckling. Because in the central area the real geometry is flatten, the area where materials are the most stressed are where there is an inflection point (fifteen centimeters approximately from the frame). We also did an inventory of connectors after mounting the prototype and we observed that neither timber battens, neither steel caps, are deformed. Only 3D printed connectors in ABS located at the area described previously are deformed.

## Conclusion

First, we verify the efficiency of interlaced structures on a flat surface in terms of number of jigs. Second, we demonstrated how this efficiency can be maintained for single curved surfaces and freeform surfaces only if the right transformation method is selected according to a specific type of surface. More specifically, the most efficient method to adapt single curved surfaces with constant radius of curvature, in terms of the relative error *R*, is the topological deformation. For the other types of single curved surfaces with non-constant radius, it is more suitable to use the compass method point by point for each wheel or the paneling method. For freeform surfaces, more specifically for the dome, the method allowing reaching a relative error *R* equal to zero is the polyhedral method. For other types of surfaces, it depends in the relative error R been required.

As well, we introduce a method to generate single curved surfaces based on the combination of two patterns. In this paper we study geometric possibilities based on four patterns selected from a large number of patterns used in the middle age Spain.

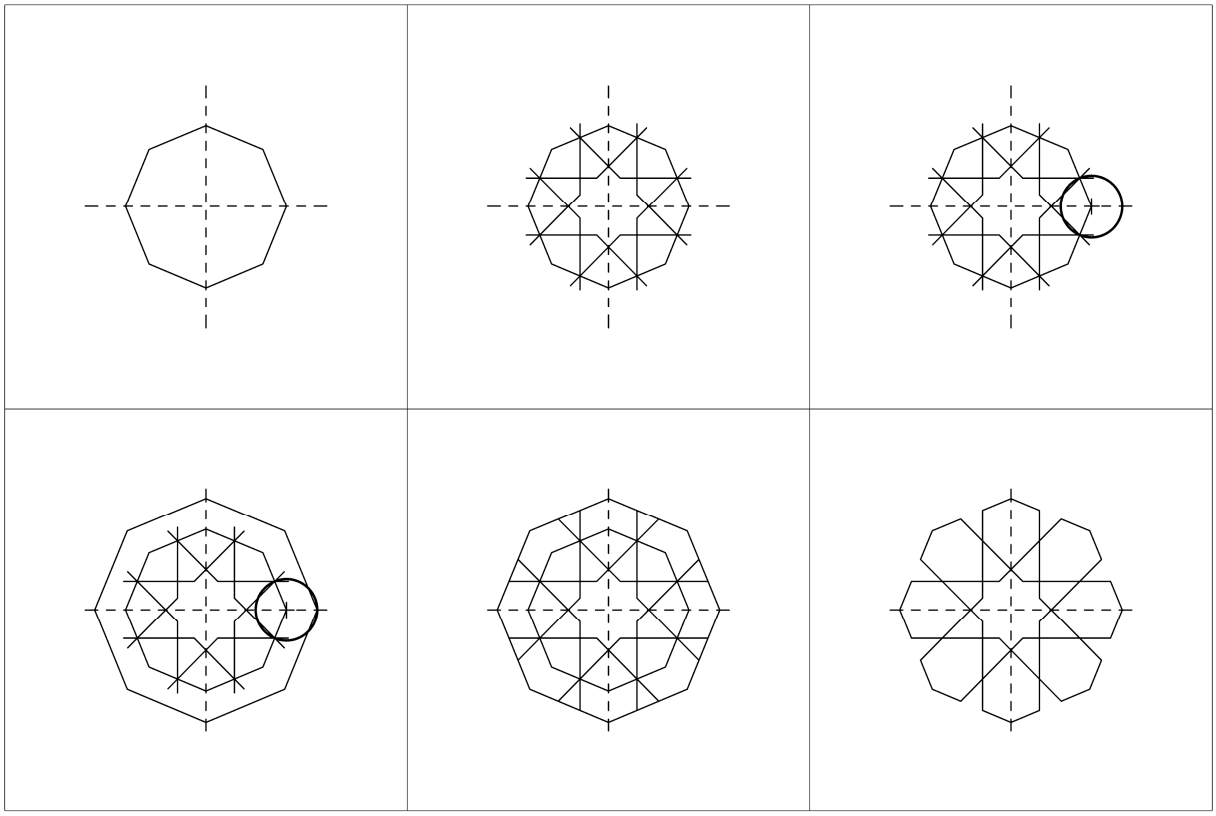

**Fig. 28**. Method to draw a wheel of eight points.

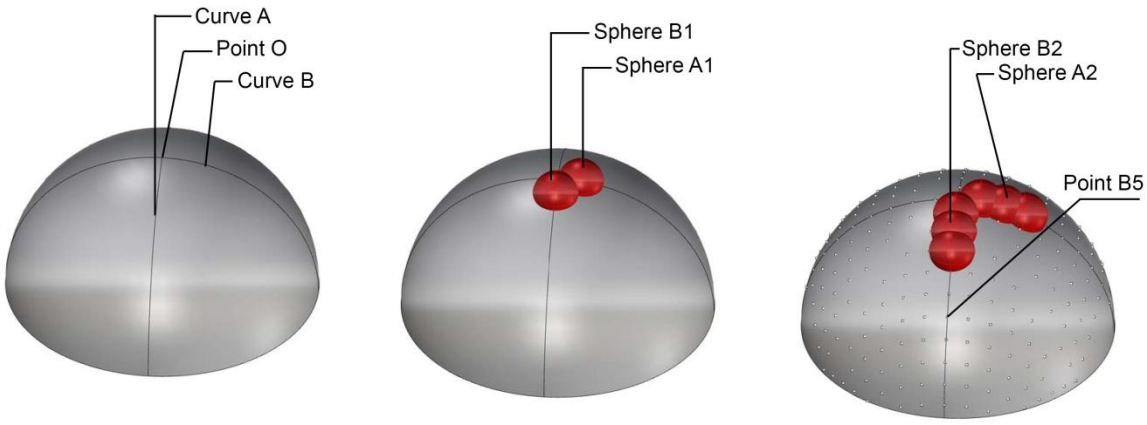


**Fig. 29**. Application of compass method in an arbitrary selected freeform surface.


**Fig. 30**. Axonometric of the nominal geometry and the real geometry.

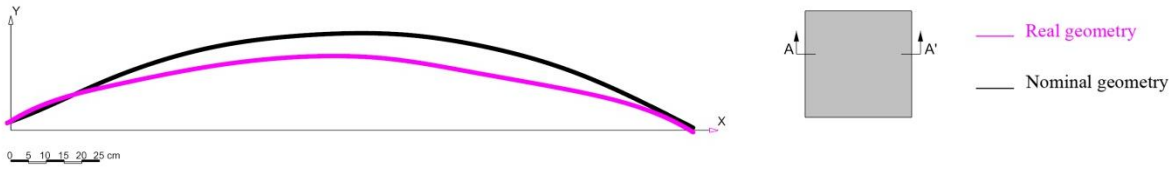


**Fig. 31**. Section A-A' of the nominal geometry and the real geometry.

Studying all other patterns and possible combinations between patterns it is a subject of research for future papers. When combining two patterns, we need to limit regions according to a criterion, in this case the minimum radius of curvature of the material. Nevertheless, this is one of the many criteria that can be applied. For example, surfaces could be split in regions according to its mechanic capacity.

## REFERENCES

Aicher S., Dill-Langer G., Höfflin L. (2001), *Effect of polar anisotropy of wood loaded perpendicular to grain*, Journal of Materials in Civil Engineering **13(1)**: 2-9.

Balinski G., Januszkiewicz K. (2016), *Digital tectonic design as a new approach to architectural design methodology*, Procedia Engineering **161**: 1504-1508.

Baverel O., Nooshin H. (2007), *Nexorades based on regular polyhedral*, Nexus Network Journal **9(2)**: 281-298.

Blaschke W., Bol G. (1938), *Geometry of the fabrics; topological questions of differential geometry* [in German], Springer, Berlin, Germany.

Bouhaya L., Baverel O., Caron J.-F. (2014), *Optimization of gridshell bar orientation using a simplified genetic approach*, Structural and Multidisciplinary Optimization **50(5)**: 839-848.

Brocato M., Mondardini L. (2012), *A new type of stone dome based on abeilles bond*, SAS International Journal of Solids and Structures **49(13)**: 1786-1801.

Brocato M., Mondardini L. (2015), *Parametric analysis of structures from flat vaults to reciprocal grids*, International Journal of Solids and Structures **54**: 50-65.

Buchelt B., Wagenführ A. (2008), *The mechanical behaviour of veneer subjected to bending and tensile loads*, Holz als Roh- und Werkstoff **66(4)**: 289-294.

Burry J., Burry M., Tamke M., Ramsgard Thomsen M., Ayres P., Pena de Leon A., Davis D., Deleuran A., Nielson S., Riiber J. (2012), *Process through practice: synthesizing a novel design and production ecology through dermoid*, Acadia **127**: 126-139.

Caicedo-Llano N. (2014), *A methodology to select a group of species among 131 tropical (Colombian) species for bowed timber applications*, Maderas. Ciencia y tecnología **16**: 245-264.

Callens S., Zadpoor A. (2018), *From flat sheets to curved geometries: Origami and kirigami approaches*, Materials Today **21(3)**: 241-264.

Duro-Royo, J. Zolotovsky K., Mogas-Soldevila L., Varshney S., Oxman N., Boyce M. C., Ortiz C. (2015), *Metamesh: A hierarchical computational model for design and fabrication of biomimetic armored surfaces*, Computer-Aided Design **60**: 14-27.

Glaeser G., Gruber F (2007), *Developable surfaces in contemporary architecture*, Journal of Mathematics and the Arts **1(1)**: 59-71.

Hoschek J. (1998), *Approximation of surfaces of revolution by developable surfaces*, CAD Computer Aided Design **30(10)**: 757-763.

Huerta S. (2007), *Oval domes: History, geometry and mechanics*, Nexus Network Journal **9(2)**: 211-248.

Lefevre B., Douthe C., Baverel O. (2015), *Buckling of elastic gridshells*, Journal of the International Association for shell and spatial structures **56(3):** 153-171.

López de Arenas D. (1912), *Brief compendium of white carpentry and alarifes treatise* [in Spanish], Albatros. Valencia, Spain

Mark R. (1996), *Architecture and evolution*, American scientist **84(4)**: 383-389.

Nuere E. (1989), *The Spanish carpentry to be assemble* [in Spanish], Ministerio de Cultura Instituto de Conservación y Restauración de Bienes Culturales, Madrid, Spain.

Otto F., Tange K., Hennicke J., Hasegawa T., 64-Weitgespannt S. (1974), *Grid shells* [in German], Institut für leichte Flächentragwerke, Stuttgart, Germany.

Rörig T., Sechelmann S., Kycia A., Fleischmann M. (2014), *Surface panelization using periodic conformal maps*, in: Philippe Block, Jan Knippers, Niloy J. Mitra, Wenping Wang (Eds.), *Advances in Architectural Geometry 2014,* 18-21 September 2014, Springer, London, United-Kingdom, pp. 199-214.

Tanguy J.- E., Mondardini L., Deleporte W., Brocato M. (2014), A proposal for a new type of prefabricated stone wall, *International Journal of Space Structures* **29**(2): 97-112.

Weinand Y., Pauly M., Robeller C., Konakovic M., Dedijer M. (2017), *Double- layered timber plate shell,* International Journal of Space Structures **32(3-4)**: 160-175.

Yamauchi H., Gumhold S., Zayer R., Seidel H.-P. (2005), *Mesh segmentation driven by Gaussian curvature,* The Visual Computer **21(8)**: 659.

**Received**: 23 January 2020 • **Revised**: 9 March 2020 • **Accepted**: 19 March 2020

Article distributed under a Creative Commons Attribution-NonCommercial-NoDerivatives 4.0 International License (CC BY-NC-ND)